Available online at www.sciencedirect.com
ScienceDirect
Cement & Concrete Composites 30 (2008) 245–252
Cement & Concrete Composites
www.elsevier.com/locate/cemconcomp

A layered finite element for reinforced concrete beams with bond–slip effects

R.S. Oliveira [a], M.A. Ramalho [b,*], M.R.S. Corrêa [b]

[a] Embraer, Av. Brigadeiro Faria Lima, 2170, 12227-901 S.J. Campos, SP, Brazil
[b] University of São Paulo, Av. Trabalhador São Carlense 400, 13566-590 – S. Carlos, SP, Brazil

Received 4 January 2006; received in revised form 21 September 2007; accepted 24 September 2007
Available online 29 September 2007

Abstract

The behaviour of reinforced concrete members is affected by the slipping of steel bars inserted in the concrete matrix. A tension-stiffening effect and crack evolution occur from the beginning of slipping; thus, the assessment of those phenomena requires the introduction of a bond–slip interaction model. This work presents a beam-layered model, including the constitutive relationships of materials and their interaction, according to the CEB-FIP Model Code 1990. To eliminate the finite element sub-division procedure, a continuous slip function is imposed into the element domain. The results are continuous descriptions of bond stress in the steel–concrete interface, as well as concrete and steel stresses along the element.

Keywords: Finite element model; Reinforced concrete beams; Bond–slip effects

1. Introduction

According to Eligehausen and Balázs [1], several factors may influence the behaviour of steel bars inserted in concrete, such as bar lug geometry and spacing, concrete strength, degree of confinement (including the amount of concrete covering the bar) and bar position inside the structural element. Identification of the factors that influence the mechanical characteristics of bonding began in the 1910s with the first studies on bonding of smooth and ribbed bars [2]. These initial studies aimed mainly to establish the relations between mean bond stress and the relative slip of the steel bars [3]. After Bresler and Bertero [4], research began to focus on the description of the variable bond stress and slip in the domain of the bar [5–7], which today are believed to be very close to the schematic illustration of Fig. 1 in the case of tensioned bar elements.

This behaviour is difficult to model because between two successive cracks (spaced at a distance S_r), owing to the slip (s), there is a strong variation in bond stress (τ) and, hence, in the axial stress in the steel bar (σ_s) and in the average value of the concrete stress (σ_c). The behaviour is even more complex in reinforced concrete beam elements, which are subjected to bending moment since, allied to the behaviour shown in Fig. 1, there is a strong variation in the position of the neutral axis in the S_r domain. Associated to this highly non-linear behaviour caused by the interaction of the materials, there are constitutive relationships for each material, which also produce physical non-linearity such as cracking, plasticity and hardening. Thus, a consistent model to represent the mechanical behaviour of reinforced concrete beams must provide a joint description, i.e. the individual behaviour of each material together with its interrelations with the other materials and boundary condition.

A finite element model that takes into account the detailed behaviour of the materials (concrete, steel) and their interaction is very useful since it provides a reliable

* Corresponding author. Tel.: +55 16 3373 9464; fax: +55 16 3373 9482.
E-mail address: ramalho@sc.usp.br (M.A. Ramalho).

0958-9465/$ - see front matter © 2007 Elsevier Ltd. All rights reserved.
doi:10.1016/j.cemconcomp.2007.09.007

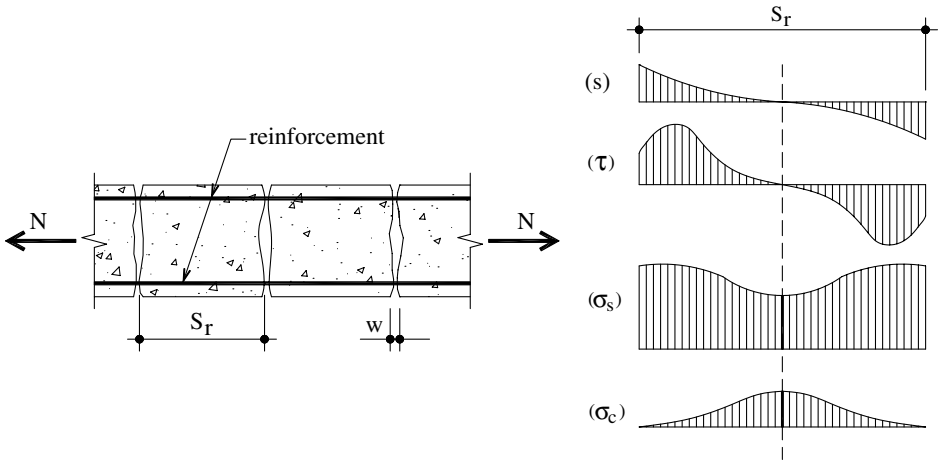

Fig. 1. Schematic slip, bond and stresses distribution along a cracked tensioned bar element.

analysis of the non-linear behaviour of the RC bending elements. It is worth noting that the simulation of the bond–slip phenomenon allows the direct representation of the tension-stiffening.

2. Material models

The constitutive relationships employed to describe the mechanical behaviour of materials as well as the interaction between steel bars and concrete are basically those proposed in CEB-FIP Model Code 1990 [8], with some slight modifications.

In compression, the behaviour of the concrete is that proposed by CEB-FIP Model Code 1990 [8] and, in tension, a linear elastic behaviour is assumed up to the strength of concrete in tension (f_{ct}). For the sake of comparison, a second model that indirectly incorporates the tension-stiffening effect [9] was also implemented. In such a model, the progressive loss of rigidity after cracking is quantified indirectly through an adaptation of the tension behaviour introducing a softening branch, which is calibrated using the α and ε_m parameters. Both the curves are illustrated in Fig. 2. The aforementioned parameters

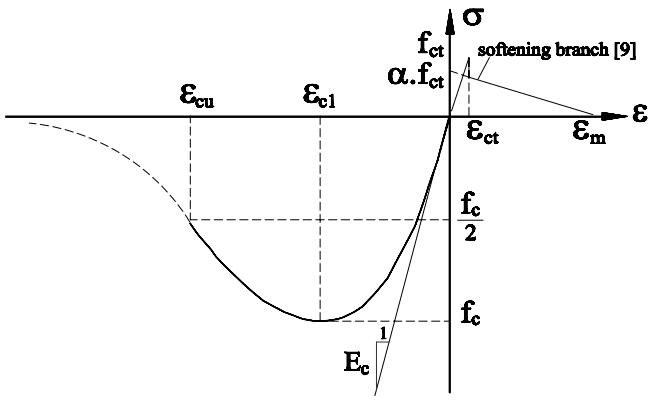

Fig. 2. Stress–strain relationship for concrete.

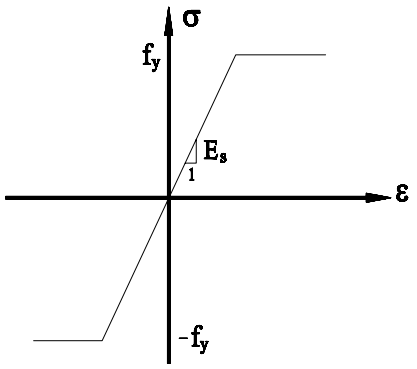

Fig. 3. Stress–strain relationship for steel.

are usually set at $0.5 \leqslant \alpha \leqslant 0.7$ and $\varepsilon_m = 0.0020$. In this case, fracture mechanics could be used to establish these values, based on energy criteria [10].

The perfect plasticity model of Fig. 3 shows the behaviour of the longitudinal reinforcement bars. The interaction between reinforcement bars and concrete is based on the diagram of Fig. 4. The parameters shown in Fig. 4 depend on the bond conditions and confinement of concrete, as established in CEB-FIP Model Code 1990 [8]. The stress–strain relationship for steel bars and the bond–slip relation-

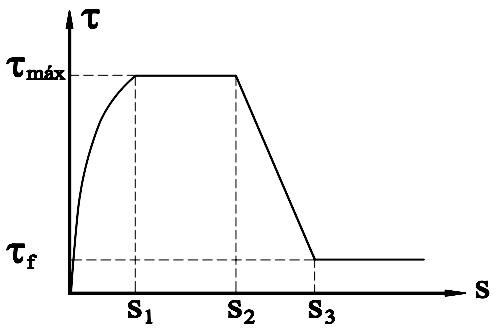

Fig. 4. Bond stress–slip relationship.

ship for the concrete–steel interface are considered independent.

3. Finite element model

3.1. Basic approach

The finite element adopted in this paper has a layered cross section, as shown in Fig. 5. Different constitutive models can be assigned to different layers allowing for the simulation of diverse materials.

Each element is defined between two consecutive potential cracks, i.e. on the length S_r showed in Fig. 1. The nodes and the integration points for an element are presented in Fig. 6.

A consistent approach was successfully introduced to analyse the distribution of stress along a steel bar inserted in a mass of concrete, and subjected to both monotonic and cyclic axial loading [11]. The bond stress–slip relations were applied to the domain of a finite element delimited by two successive cracks. Boundary conditions on steel stress

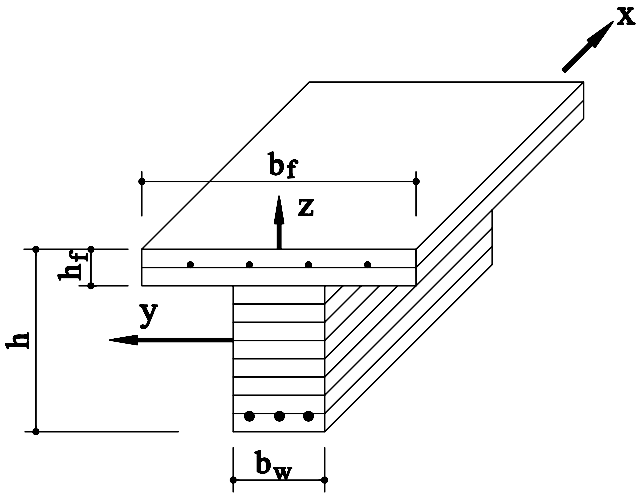

Fig. 5. The layered finite element.

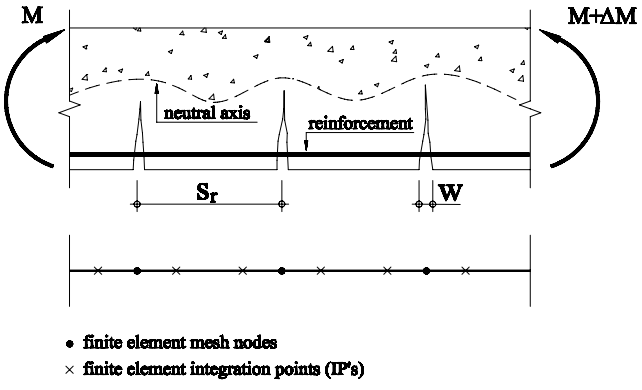

Fig. 6. Nodes and integration points of the finite element.

($\sigma_s = N/A_s$), concrete stress ($\sigma_c = 0$), and on their interface ($\tau = 0$, and $s = s_{max} \neq 0$) were established in the cracked sections, giving rise to an iterative procedure that sequentially established the conditions of axial force equilibrium in the cross section as a whole and in the steel bars in each sub-element (sub-domain of the element).

The description of the stress variables in each sub-element depends on the relative slip between the steel bars and the surrounding concrete, given by the difference in longitudinal displacements between them:

$$\frac{ds(x)}{dx} = \frac{d[u_s(x) - u_c(x)]}{dx} = \varepsilon_s(x) - \varepsilon_c(x) \tag{1}$$

where $u_s(x)$ and $u_c(x)$ are, respectively, the longitudinal displacements of the steel bars and the portion of concrete surrounding them, ε_s and ε_c represent, respectively, the strains in the longitudinal reinforcement and in the surrounding tensioned concrete.

Assuming that the bond stress τ is uniformly distributed ($\bar{\tau}$) in each δx sub-domain, the values in the $i+1$ section are determined from the values established in the i section, using the finite differences method:

$$\sigma_{s,i+1} = \sigma_{s,i} - \frac{4}{\phi} \cdot \tau_i \, \delta x \tag{2}$$

$$(\sigma_{c,i} - \sigma_{c,i+1}) \cdot A_c = (\sigma_{s,i} + 1 - \sigma_{s,i}) \cdot A_s \tag{3}$$

$$s_{i+1} = s_i - (\varepsilon_{s,i+1} + \varepsilon_{s,i}) \cdot \frac{\delta x}{2} + (\varepsilon_{c,i} + 1 + \varepsilon_{c,i}) \cdot \frac{\delta x}{2} \tag{4}$$

where ϕ is the diameter of the longitudinal steel bar, A_c is the area of concrete in compression and A_s is the area of the steel bar.

3.2. Proposed modifications

Based on the above-described idea, Manfredi and Pecce [12] used the model to the analysis of reinforced concrete elements subjected to bending, introducing another equilibrium condition to each sub-element concerning the bending moment:

$$\int_{A_c} \sigma_c \cdot z_c \cdot b_w \cdot dz + A_s \cdot \sigma_s \cdot z_s = M(x) \tag{5}$$

where z_c is the distance from the concrete resultant to the neutral axis, b_w is the cross section width, z_s is the distance from the reinforcement to the neutral axis and $M(x)$ is the bending moment.

Based on theoretical and experimental observations [12–14], a new approach is proposed based on a linear field for the slip along the transmission length (l_t), from the crack to the centre of the finite element. Of course the adopted procedure may produce results that are sensitive to the finite element mesh and an example will be presented later in order to clarify these aspects. The functions describing bond stress, and, the consequent steel stresses, emerge as a result of this adopted slip function. After that, by imposing the axial force equilibrium, the stress for the concrete

can be established at each x coordinate point of the domain.

Finite elements are defined between two possible cracking sections after the start-up of loading, which implies that their two nodes must coincide with these sections. The cracks will occur in the sections where stress in concrete reaches the strength of concrete in tension (f_{ct}). The distance between cracks (S_r) can be evaluated using the semi-empiric formulations provided by codes or imposing the same distance between successive stirrup locations [12]. A suggestion could be simply taking the smallest of them. One-dimensional constitutive relationships are applied to a finite element layered model.

Since non-linear constitutive relations are adopted, an incremental iterative procedure is employed in the solution of the global equation system. At each iteration the boundary conditions at the cracks (nodes) are established through the equilibrium of axial force ($N = 0$). In these sections, the contribution of the tensioned concrete is also taken into account, as shown in the diagram of Fig. 2, only in its ascending part, up to the value of f_{ct}. Note that the explicit introduction of the bond–slip relation allows direct evaluation of the tension-stiffening effect with the consequent reduction of the steel strain along the steel bar between two cracks. It should be pointed out that the equilibrium of axial force established will certainly lead to an unbalanced portion of the bending moment (ΨM), to be integrated in order to establish the residual load increment, applied to the subsequent iteration:

$$N = b \cdot \int_{-h/2}^{h/2} \sigma_c \cdot dz + \sum_{k=1}^{n_b} \sigma_s \cdot A_{s,k} = 0 \tag{6}$$

$$\Psi M = \left(b \cdot \int_{-h/2}^{h/2} \sigma_c \cdot z_c \cdot dz + \sum_{k=1}^{b} \sigma_s \cdot z_s \cdot A_{s,k} \right) - M(x) \tag{7}$$

where b may take on b_w or b_f values, depending on the position of the layer analysed, web or flange, respectively. $A_{s,k}$ corresponds to the area of each of the n_b bars that comprise the longitudinal reinforcement, h corresponds to the height of the beam element, while z_c and z_s represent, respectively, the position of each concrete layer or bar of the longitudinal reinforcement in relation to the neutral axis. In the present paper the model is applied to flexure-only beams, although it can be extended easily to the case with axial forces, with an appropriate change in Eq. (6).

The slip value in the section of the first crack ($s_{max,1}$) is approximated by imposing the $\delta x = l_{t,1}$ and $\varepsilon_c = \varepsilon_{ct}$ conditions to Eq. (1)

$$s_{max,1} = l_{t,1} \cdot (\varepsilon_{s,1} - \varepsilon_{ct}) = l_{t,1} \cdot \left(\frac{\sigma_{s,1}}{E_s} - \varepsilon_{ct} \right) \tag{8}$$

where ε_{ct} is the strain corresponding to the maximum tension stress (f_{ct}) and $l_{t,1}$ the transmission length. The slip function may, therefore, be described in the element's domain as

$$s(x_1) = s_{max,1} \cdot \left(1 - \frac{x_1}{l_{t,1}} \right) \tag{9}$$

The same procedure is repeated for the second crack that delimits the finite element. It is also important to note that this model, contrary to Manfredi and Pecce [12], does not require the existence of two consecutive cracks to carry out the analysis of the element, since this method does not require verification of the convergence at the second crack. Once a description has been obtained of the two slip functions for the finite element nodes, both directly dependent on the axial stress of the reinforcement established at these nodes, the bond stress function and the stress in the reinforcement along the transmission length are immediately obtained, based on the relation proposed by the CEB-FIP 1990 Model Code (Fig. 4) applied to the integral equation:

$$\sigma_{s,x} = \sigma_{s,node} - \frac{4}{\phi} \cdot \int_0^x \tau(x) \cdot dx \tag{10}$$

Note that $l_{t,1}$ and $l_{t,2}$ can be assessed by the integration of the bond–slip diagram of Fig. 4 taking into account Eqs. (9) and (10), with $s_{s,x} = 0$.

Fig. 7 shows three different situations related to the sum of the transmission lengths ($l_{t,1} + l_{t,2}$) after cracking. The situations in which this sum is inferior or equal to S_r (a, b) are perfectly assimilated by the model. The third situation, according to Martins [13], can be modelled by the fictitious superposition of one slip function over another,

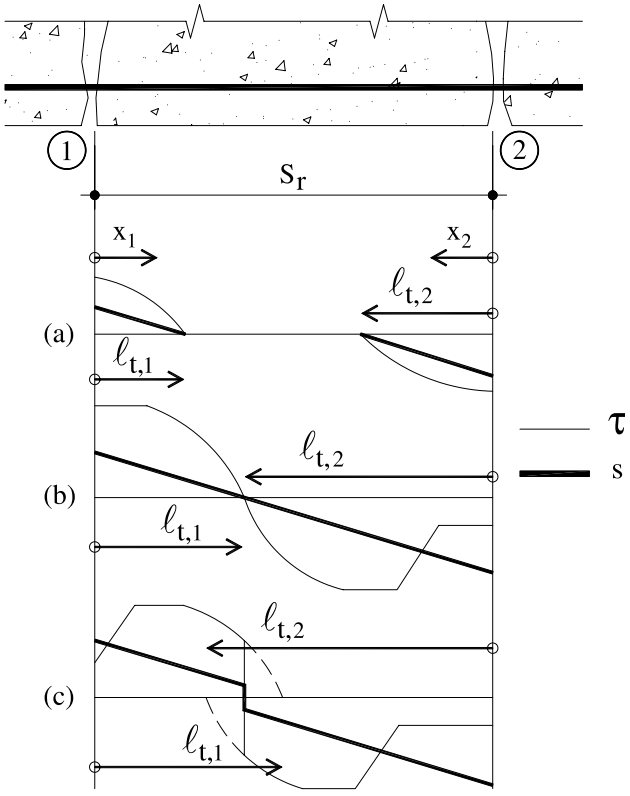

Fig. 7. Bond–slip with loading increment.

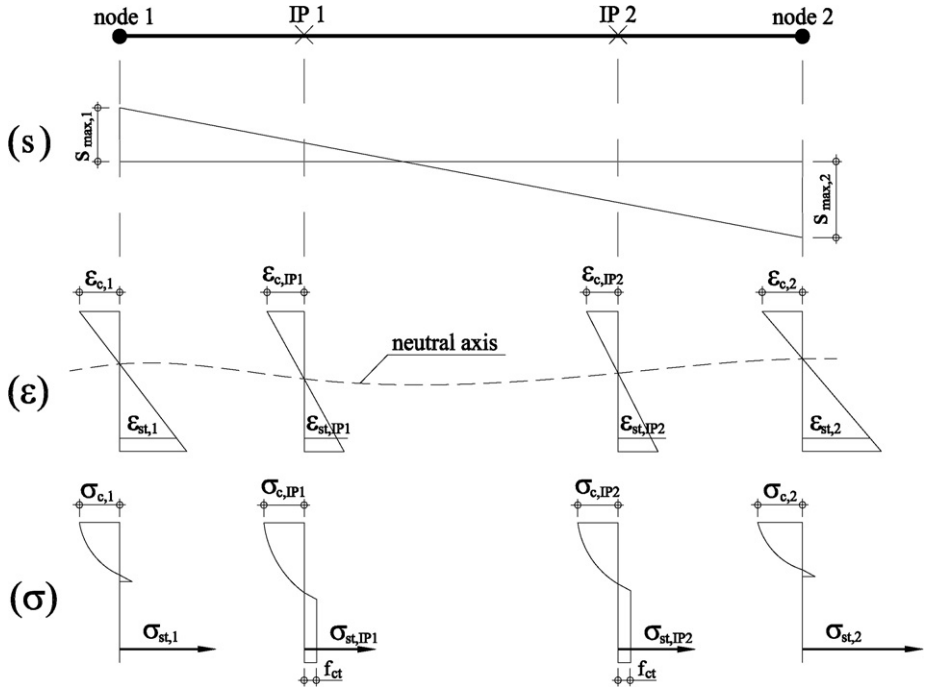

Fig. 8. Element strain–stress states.

characterizing a point of discontinuity that divides the influence limits of the two cracks.

Once a description of the bond stress is obtained and, consequently, of the steel bars stresses, the stress state in the concrete is well established at each iteration and at any point (x) in the domain, imposing the equilibrium of axial force ($N = 0$). The internal forces ($M, N = 0$) are assessed by discrete integration over the layers of concrete and the discrete steel bars in the cross section, establishing the neutral axis. The element's residual forces are determined by the difference between external load and internal forces, which is similar, in this case, to the integration of ΨM over the element domain, Owen and Hinton [15]. Among many other integration rules, the Gauss–Lobatto method seems to be more convenient, allowing one to compute the unbalanced forces at the element's nodes and at determined internal sections, which correspond to the integration points (IPs).

The tensile concrete stresses are always limited to the f_{ct} value, i.e. at any section they can vary from zero up to f_{ct} (see Fig. 8). At nodes, the cross section may be considered cracked and in this case the tensile concrete stress drops from f_{ct} to zero, simulating the brittle behaviour. At the IPs, if the tensile concrete stress reaches the value of f_{ct}, it is kept constant, since the appearance of secondary cracks is not considered in this model, Broms [14].

It can be noted, in Fig. 8, that the strains of the longitudinal reinforcement at the IPs are not necessarily equal to the strains of the concrete layers located, respectively, at the same positions. This is a consequence of the fact that the stress in the reinforcement is described by the slip function, which depends on both the nodal value of the reinforcement stress and the bond stress–slip relationship. In most cases, this gives rise to specific strains that differ from those occurring in the concrete layer adjacent to the reinforcement, according to Bernoulli's hypothesis (plane sections remain plane). This fact applies to both higher and lower values than those obtained considering the linear strain diagram for concrete, which is natural, since the proposed model allows for a slip to be represented.

4. Comparisons with experimental results

The reliability of the model proposed in this paper has been tested through many comparisons with experimental and theoretical results. One of these experiments Burns and Siess [16], carried out on a simply supported beam, whose experimental results are considered very reliable, was also used by Kwak and Filippou [17] to check a numerical model. Such a model refers to the insertion of a steel element into an eight-node serendipity plate element. The behaviour of the concrete is non-linear and governed by the Kupfer criterion. The steel bars inserted in the plate element are also modelled according to a non-linear one-dimensional model with isotropic positive hardening.

In this work, the beam was divided by means of 16 finite elements. The cross section was divided into 10 concrete layers superimposed over the longitudinal reinforcement, as it is shown in Fig. 9. A longitudinal reinforcement corresponding to 9Ø12 mm and a bond stress–slip diagram were adopted, as illustrated in Fig. 10. The total load of 163.3 kN was divided into 10 increments of 16.33 kN each. Finally, the mechanical properties of the involved materials are summarized in Table 1.

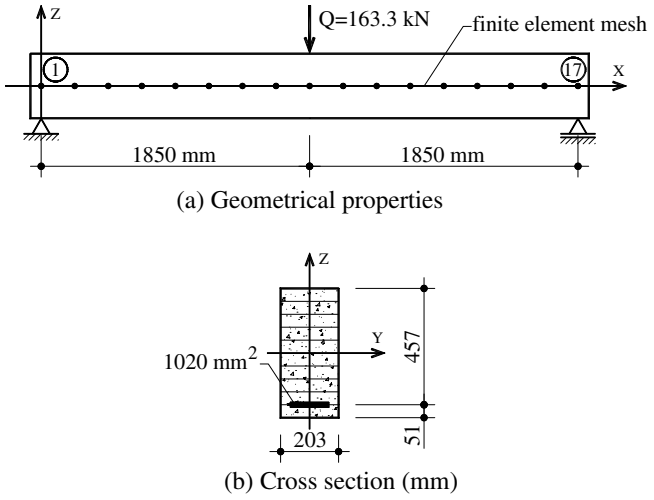

Fig. 9. Beam and finite element mesh – example 1.

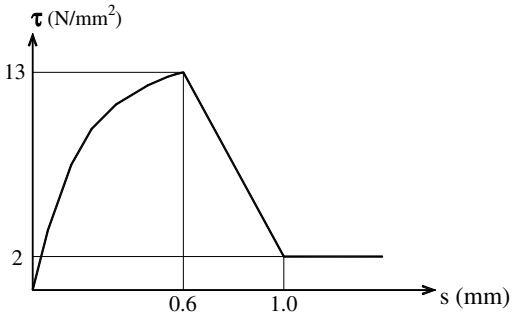

Fig. 10. Bond stress–slip relationship – example 1.

Table 1
Material properties – example 1

E_c (N/mm^2)	E_s (N/mm^2)	f_c (N/mm^2)	f_{ct}[a] (N/mm^2)	f_y (N/mm^2)	ρ (%)
26,700	207,400	33.90	3.60	316.0	0.99

[a] Value adopted based on the CEB-FIP MC90.

The load–deflection relationships obtained by this model are shown in Fig. 11. The experimental results obtained by Burns and Siess [16] are also given, in addition to results presented by Kwak and Filippou [17]. The results by an empirical model, Figueiras [9], are also included considering both the extreme values indicated for the α variable. The obtained results are very close to the experimental ones, showing the good accuracy of the present model.

One very important feature of non-linear models applied to the analysis of structural reinforced concrete elements is the problem of the finite element mesh size. Especially for the adopted procedure the results can be sensitive to element length because of the distance between cracks. In order to study this aspect, the same example was analysed by two other meshes, composed of 8 and 32 finite elements. The results illustrated in Fig. 12 indicate the model's satisfactory behaviour, since the three obtained responses presented no significant differences between the 16 and 32 element meshes. As for the eight element mesh, it is excessively poor for this kind of problem and even so the results are reasonable for engineering purposes.

Finally, it is important to point out that 10 layers for the cross section is really enough, even when the non-linearity effects are very significant. For the presented example the increasing of the number of layers from 10 to 20 produced almost the same results for the midspan displacement. A similar conclusion is presented in Figueiras [9].

The model also allows one to obtain the results of the crack widths at the nodes of the finite element mesh. Fig. 13 shows the results of the beginning of beam cracking (with a load equivalent to 30% of the ultimate load), and the cracking evolution toward the supports, as well as their growth under incremental loading (up to 80% of the total foreseen load), for 16 and 32 element meshes. Note that the different meshes produce similar crack distributions. This kind of information is very important in the design of structural reinforced concrete elements, specifically in

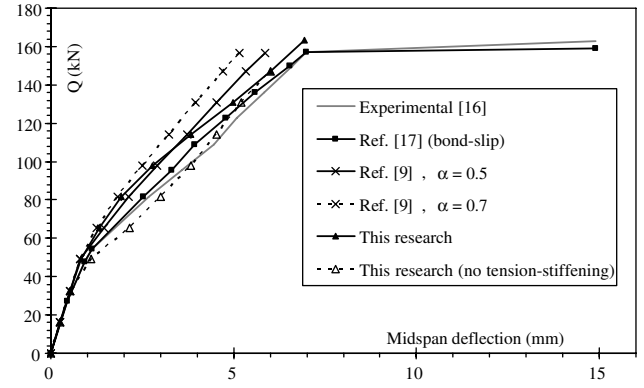

Fig. 11. Deflections for the beam – example 1.

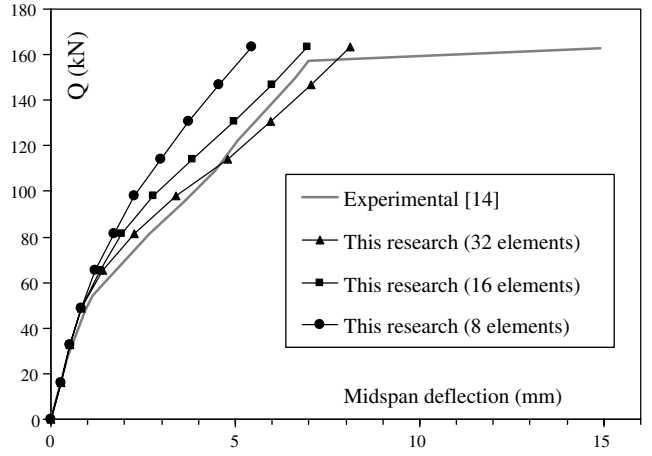

Fig. 12. Mesh size effect – example 1.

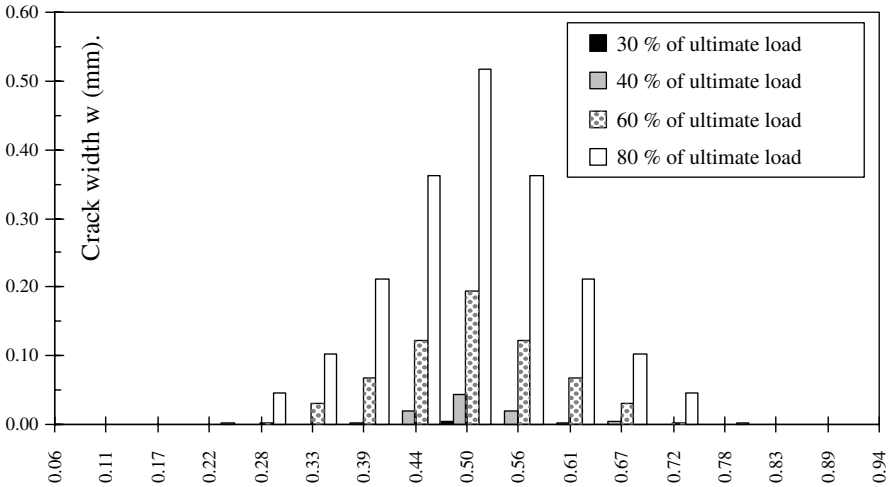

(a) 16 elements

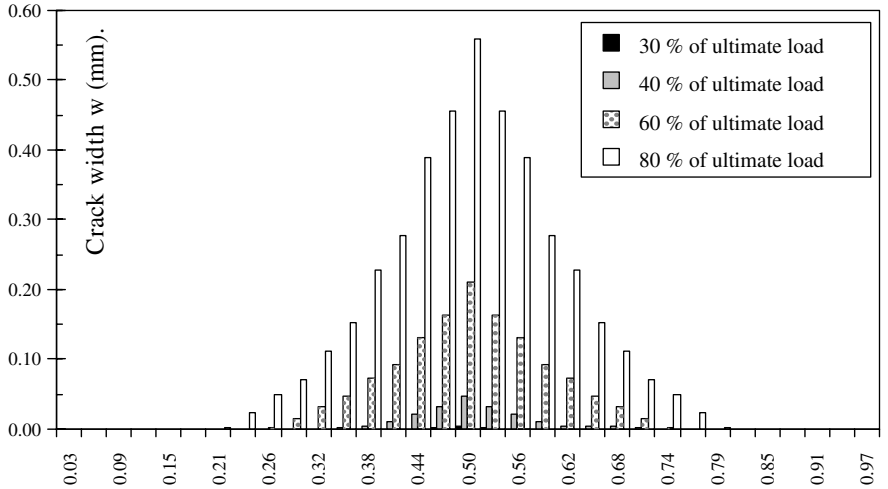

(b) 32 elements

Fig. 13. Cracking evolution with load increment – example 1.

checking their service limit state with respect to crack widths.

Another example is presented, in order to show the post-yield behaviour and the capabilities of the present model. Fig. 14 shows the simply supported beam with its geometric features and the finite element mesh used to simulate the experiment carried out by Alvares [18].

Table 2 summarizes the properties of the materials as measured by the referred author. The beam was simulated by 12 finite elements and the cross sectional area was divided into 10 concrete layers superimposed to the steel bars, Fig. 14. The load was applied by means of 10 equal increments. Fig. 15 shows the load–deflection relationships obtained with the present model and the experimental results for the two specimens of the same beam. The theoretical results, especially those regarding the use of Mazars [19] uni-axial damage model for the concrete, are similar to the experimental ones. Note that, in this case, the inflection

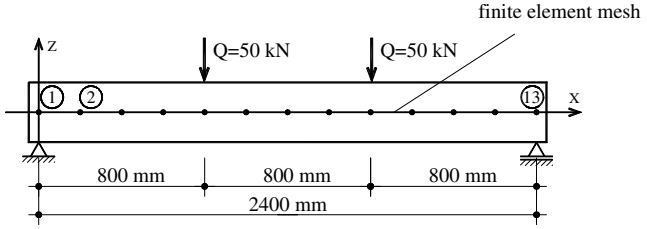

(a) Geometrical properties

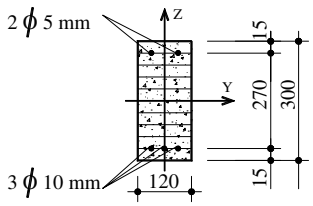

(b) Cross section (mm)

Fig. 14. Second beam and finite element mesh – example 2.

Table 2
Material properties – example 2

Concrete		Steel
Elastoplastic	Damage model[a]	
$\varepsilon_{c1} = 0.0032$	$\varepsilon_{d0} = 0.00007$	–
$\varepsilon_{cu} = 0.0070$	$A_c = 0.85$	–
$\varepsilon_m = 0.0020$	$B_c = 1050$	–
$f_c = 25.5\ \text{N/mm}^2$	$A_T = 0.995$	$f_y = 500\ \text{N/mm}^2$
$f_{ct} = 2.044\ \text{N/mm}^2$	$B_T = 8000$	–
$E_c = 29{,}200\ \text{N/mm}^2$		$E_s = 196{,}000\ \text{N/mm}^2$

[a] ε_{d0}, A_c, B_c, A_T, B_T – experimental parameters for the Mazars [19] damage model.

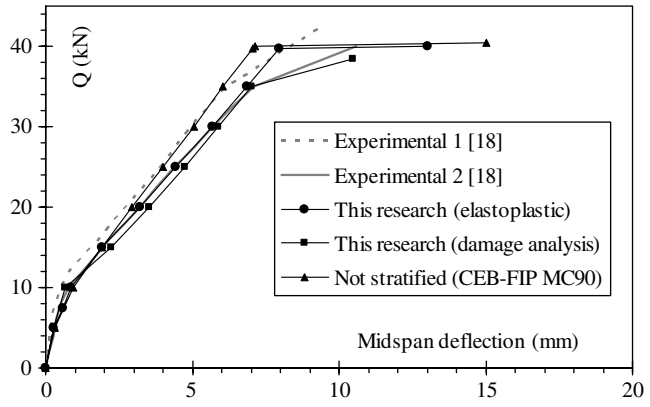

Fig. 15. Deflections for the beam – example 2.

due to the steel yielding is well represented by the present model, which also shows a similar slope for the post-yield behaviour regarding the second tested beam.

5. Conclusions

This paper introduces a new methodology for a consistent approach to the slip phenomenon affecting the structural behaviour of a beam element. The methodology allows for a continuous description of several variables involved in determining the phenomenon, from the imposition of a linear field to the relative slip between reinforcement bars and concrete along the domain of each element.

This methodology offers several advantages in relation to what is currently being used. Most of the models available in the scientific literature approach the problem through the finite differences applied to a sub-partitioned finite element. Besides additional computational effort, the produced results are discontinuous in the finite element domain and constant in the domain of each sub-element. This model produces continuous and variable results throughout the element's domain. The results obtained from the present model can be considered reliable in view of the fact that they came very close to the experimental results as well as to those obtained by other authors. A brief study of the problem of finite element mesh size revealed that the behaviour is only slightly influenced by this effect. Hence, the proposed model applied to practical problems of structural engineering should produce good results.

References

[1] Eligehausen R, Balázs GL. Bond and detailing. In: Proceedings of the colloquium on the CEB-FIP MC90, Rio de Janeiro, 1991. p. 213–61.
[2] Abrams DA. Test of bond between concrete and steel. Univ Illinois Bull 1913;11(15):1–238. paper 71.
[3] Glanville WH. Studies in reinforced concrete-bond resistance, Building Research Technical Paper 10, 1930.
[4] Bresler B, Bertero V. Reinforced concrete prism under repeated load. In: Proceedings of the RILEM symposium on the effects of repeated loading on materials and structural elements, Mexico, 1966.
[5] Nilson AH. Nonlinear analysis of reinforced concrete by the finite element method. ACI J 1968;65(9):757–66.
[6] Mirza SM, Houde J. Study of bond stress–slip relationships in reinforced concrete. ACI Struct J 1979;76(1):19–46.
[7] Eligehausen R, Popov EP, Bertero VV. Local bond stress–slip relationships of deformed bars under generalized excitations. Report UCB/EERC 83–23, Earthquake Engineering Research Centre, Berkeley, University of California, 1983.
[8] Comité Euro-International du Béton CEB-FIP Model Code 1990: Final draft, CEB Bulletin D'Information, 1990. p. 203–5.
[9] Figueiras JA. Ultimate load analysis of anisotropic and reinforced concrete plates and shells, PhD thesis. Swansea, University College of Swansea, 1983.
[10] Ranjbaran A, Phipps ME. DENA: a finite element program for the non-linear stress analysis of two-dimensional, metallic and reinforced concrete, structures. Comput Struct 1994;51(2):191–211.
[11] Tassios TP, Yannopoulos PJ. Analytical studies on reinforced concrete members under cyclic loading based on bond stress–slip relationships. ACI J 1981;78(3):206–16.
[12] Manfredi G, Pecce M. A refined RC beam element including bond–slip relationship for the analysis of continuous beams. Comput Struct 1998;69:53–62.
[13] Martins PCR. Bond stress–slip influence on flexural behaviour of PPC elements. In: Proceedings of the colloquium on the CEB-FIP MC90, Universidade Federal do Rio de Janeiro, Rio de Janeiro, 1991. p. 263–88.
[14] Broms BB. Crack width and crack spacing in reinforced concrete members. ACI J 1965;62(10):1237–55.
[15] Owen DRJ, Hinton E. Finite elements in plasticity: theory and practice. Swansea: Pineridge Press Ltd.; 1980.
[16] Burns NH, Siess CP. Load–deformation characteristics of beam-column connections in reinforced concrete. University of Illinois at Urbana, SRS 234, 1962.
[17] Kwak HG, Filippou FC. Nonlinear FE analysis of R/C structures under monotonic loads. Comput Struct 1997;65(1):1–16.
[18] Alvares MS. Modelling of concrete: formulation, parametric characterization and application of the Finite Element Method, MSc thesis. São Carlos, University of São Paulo, 1993.
[19] Mazars J. Application de la mécanique de l'endommagement au comportement non lineaire et à la rupture du béton de structure. Thése de Doctorat d'État, Université Paris 6, 1984.